

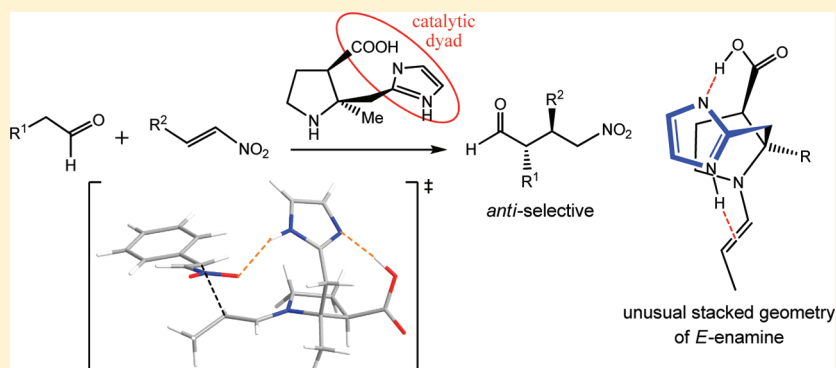
β -Amino Acid Catalyzed Asymmetric Michael Additions: Design of Organocatalysts with Catalytic Acid/Base Dyad Inspired by Serine Proteases

Hui Yang and Ming Wah Wong*

Department of Chemistry, National University of Singapore, 3 Science Drive 3, Singapore 117543

S Supporting Information

ABSTRACT:



A new type of chiral β -amino acid catalyst has been computationally designed, mimicking the enzyme catalysis of serine proteases. Our catalyst approach is based on the bioinspired catalytic acid/base dyad, namely, a carboxyl and imidazole pair. DFT calculations predict that this designed organocatalyst catalyzes Michael additions of aldehydes to nitroalkenes with excellent enantioselectivities and remarkably high *anti* diastereoselectivities. The unusual stacked geometry of the enamine intermediate, hydrogen bonding network, and the adoption of an *exo* transition state are the keys to understand the stereoselectivity.

INTRODUCTION

In the past decade, we have witnessed an unprecedented growth and impact of organocatalysis in asymmetric reactions.¹ The discovery of intermolecular proline-catalyzed aldol reactions by List, Lerner, and Barbas represents a major development of enamine catalysis.² Nowadays, proline is well accepted as a prototypical example of organocatalysis.¹ In asymmetric proline-catalyzed reactions, proton transfer from the proline's carboxyl group to corresponding proton acceptor is crucial to determine the final stereoselectivity.³ Thus, it would be highly desirable that proton transfer in catalysis could occur in a controllable manner.

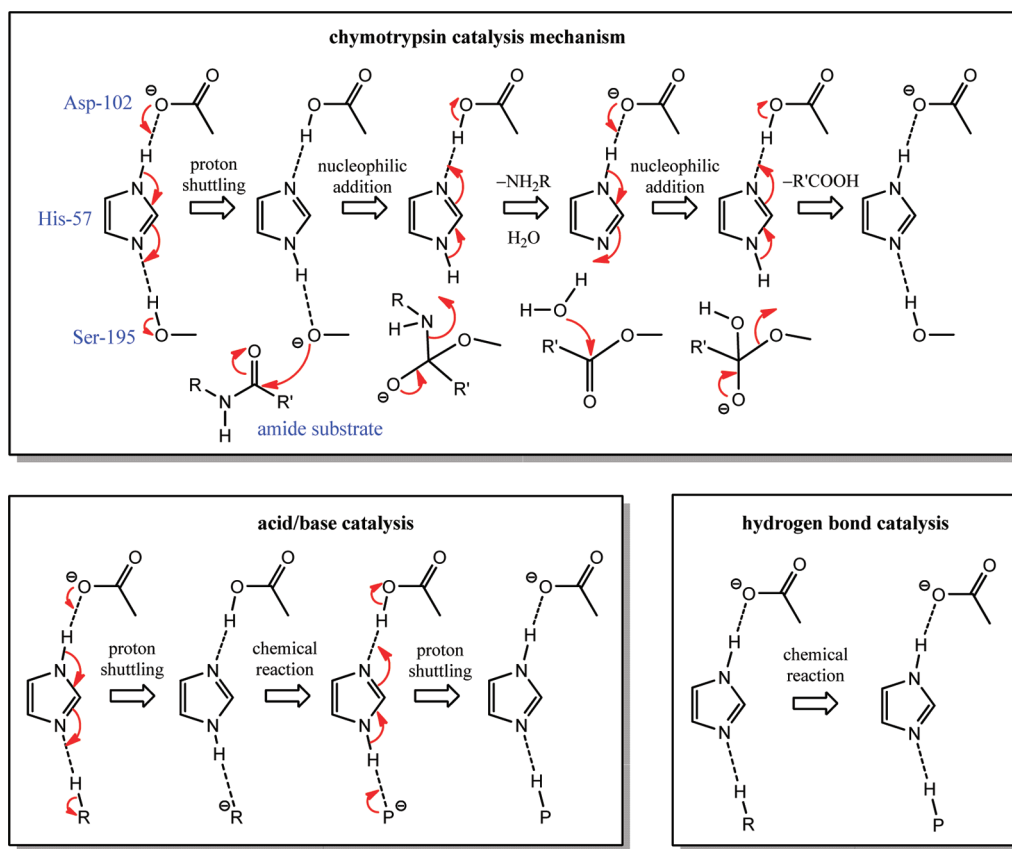
Enzymes, nature's catalysts, are major source of inspiration for design of new organocatalysts with high catalytic efficiency and stereoselectivity. Many important biochemical transformations involve proton transfer. In an environment full of polar hydrogen and protons, it would be intriguing to know how nature controls proton delivery so precisely that a proton would be transported only to the desired location. One of the most well established enzymatic catalysis involving proton transfer is the hydrolysis of peptide bonds by serine proteases, e.g., chymotrypsin.⁴ The catalytic center inside the active site of chymotrypsin is a triad of amino acid residues, aspartic acid, histidine, and serine, which forms a highly ordered 3D structure that shuttles proton between

residues Asp-102 and Ser-195 through an imidazole bridge in His-57.⁴ We envisage that the mode of enzyme catalysis in chymotrypsin (Scheme 1), or serine proteases in general, can be extended to organic transformations using general acid/base or hydrogen bond catalysis. In the catalytic triad of chymotrypsin, the serine residue acts as an active nucleophile in the nucleophilic addition step and a leaving group in the subsequent deacylation step, while the histidine and aspartic acid residues serve as an acid/base pair for the proton shuttling steps and hydrogen bonding network for charge transfer (Scheme 1). The carboxyl/imidazole pair forms a coordination dyad, linked by hydrogen bond, and is conserved in all reaction steps. Thus, the two functional groups generic to implement either acid/base or hydrogen bond catalysis are the carboxyl group, as in the side chain of aspartic acid, and the imidazole ring, as in the side chain of histidine. The side chain of the serine residue could be replaced by a proton or hydrogen-bond donor from the reaction substrate of interest. The carboxyl/imidazole pair, as an acid/base dyad, provides a proton and thus serves as a Brønsted acid catalyst. This concept of catalytic dyad, which forms a charge

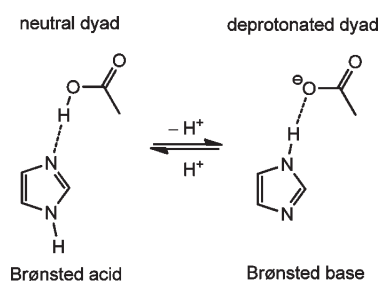
Received: June 2, 2011

Published: August 01, 2011

Scheme 1. Catalytic Dyad in Chymotrypsin Catalysis Mechanism, Acid/Base Catalysis, and Hydrogen Bond Catalysis



Scheme 2. Proposed Carboxyl/Imidazole Dyad As Brønsted Acid and Base

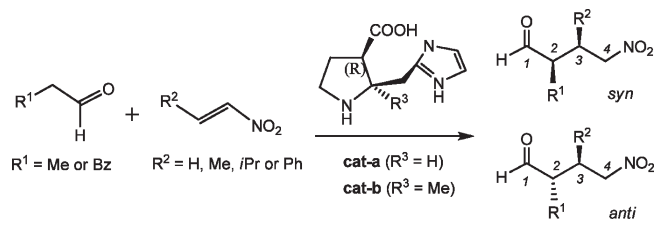


relay network, in various modes of catalysis, is illustrated in Scheme 1. Since imidazole is amphoteric, i.e., it can function as both an acid and a base, the catalytic dyad as a whole can be either in an acid form, which serves as a Brønsted acid, or the conjugate base form, which serves as a Brønsted base (see Scheme 2). As a consequence, the catalytic acid/base dyad could provide a unique function in shuttling protons back and forth in a sequence of reaction steps, as shown in the catalysis mechanism of chymotrypsin. It should be noted that in biochemistry, catalytic dyads of various combinations of amino acid residues⁵ are known in literature. However, to the best of our knowledge, no application of a catalytic dyad in organocatalysis either experimentally or theoretically has been reported in the literature so far. We envision that using a catalytic dyad of carboxyl/imidazole may

provide two distinct advantages: (1) enhanced Brønsted acidity/basicity of imidazole via hydrogen bond to carboxyl group and (2) a means to orient and position imidazole and hence fine-tune its hydrogen bonding properties.

With the tremendous advances in computing power and methodology development over the past decades, it has become practical to design novel catalysts purely *in silico*. Several such attempts have been reported in the recent years.⁶ In fact, some of the theoretically designed novel catalysts have been verified by experiments with good satisfaction.⁷ In this paper, we report our attempt to design novel organocatalysts computationally by implementing the concept of a catalytic dyad. We propose the use of a carboxyl/imidazole dyad as a Brønsted acid/base, which can be applied to both general acid/base catalysis as well as hydrogen bond catalysis. Several common and recently reported organic templates have been considered, and we have chosen pyrrolidine as the base skeleton due to its rigidity of structure, high nucleophilicity of its derived enamines,⁸ ease of synthesis and its successful application in many organocatalytic reactions. Hence, our designed catalyst is a simple β -amino acid with an imidazole substituent in the α position and a carboxyl group in the β position (with *R* chirality) (Scheme 3). To test our hypothesis, we have investigated computationally the asymmetric nitro-Michael reaction of aldehyde as an example of hydrogen bond catalysis (Scheme 3). The catalytic mechanisms of asymmetric Michael additions using organocatalysts, e.g., proline and its derivatives, have been studied extensively by theory and experiment.⁹ It is believed that the high observed enantioselectivities

Scheme 3. Michael Additions between Selected Aldehydes and Nitroalkenes Using Designed β -Amino Acid Based Catalysts *cat-a* and *cat-b*



are attributed to the formation of highly organized transition states with a hydrogen bonding framework.¹⁰

COMPUTATIONAL METHODS

Equilibrium structures and transition states were fully optimized using the M06-2X¹¹ density functional method together with the 6-31G** basis set. The M06-2X functional was chosen as this empirical functional is better suited than normal hybrid DFT methods (e.g., B3LYP) in handling kinetics, thermodynamics, and noncovalent interactions such as N–H $\cdots\pi$ interaction.¹¹ Frequency analyses were performed on the M06-2X/6-31G** optimized geometries to confirm the nature of the stationary points as equilibrium structures (with all real frequencies) or transition states (with only one imaginary frequency). Higher-level relative energies were obtained through MP2/6-311+G** single-point calculations. Unless otherwise noted, the relative energies reported in the text correspond to relative free energies at 298 K (ΔG_{298}), computed at MP2/6-311+G**/M06-2X/6-31G**. The effect of solvation was examined by an implicit polarizable continuum model (PCM).¹² Charge density analysis was performed using the natural bond orbital (NBO)¹³ approach based on the M06-2X/6-31G** wave function. All calculations were performed using the Gaussian 09 suite of programs.¹⁴

RESULTS AND DISCUSSION

Cat-a-Catalyzed Michael Addition. A prototypical designed catalyst *cat-a* ($R^3 = H$) was tested initially for its efficiency as a catalyst for asymmetric Michael addition of propanal to nitrostyrene ($R^1 = Me$ and $R^2 = Ph$, Scheme 3). It is well established that catalytic Michael additions using amine catalysts proceed via an enamine mechanism.^{8,15} The active enamine intermediate serves as a nucleophile in addition to a Michael acceptor substrate. The C–C bond-formation step is the rate-determining step and governs the product stereoselectivity. As with other organocatalysts reported in literature,⁸ *cat-a* favors the formation of *syn* products, with excellent predicted enantioselectivity and diastereoselectivity (entry 1, Table 1). The *E* configuration is the preferred conformation of the enamine intermediate (**enam-a**). In the C–C bond-forming transition states, the proposed catalytic acid/base dyad is clearly seen (Figure 1).

Initially, we hypothesized that the hydrogen bonding network of the catalyst moiety would have a deterministic effect of directing nitrostyrene attack from the same face, i.e., the *si* face of enamine (see proposed transition state in Figure 1), resulting in the formation of a *syn*-Michael adduct. To our disappointment, the optimized geometry of the lowest-energy transition state, **TS1-RS** (Figure 1), does not follow our expectation, even though the catalyst still favors a *syn* product. On the basis of the calculated transition state corresponding to our proposed model

Table 1. Calculated Relative Energies (ΔG_{298} and ΔH_{298} , kJ mol⁻¹) of the Four Transition States Leading to the Four Stereoisomeric Products^a for Various Michael Additions Catalyzed by *cat-a* and *cat-b* (Scheme 3)

entry	catalyst	R ¹	R ²	TS-SS	TS-RR	TS-SR	TS-RS
ΔG_{298}							
1	<i>cat-a</i>	Me	Ph	19.7	40.4	34.8	0.0
2	<i>cat-b</i>	Me	Ph	0.0	25.2	23.5	20.1
3 ^b	<i>cat-b</i>	Me	H	0.0	25.4	26.7	26.2
4	<i>cat-b</i>	Me	Me	0.0	25.9	28.9	27.8
5	<i>cat-b</i>	Me	<i>i</i> Pr	0.0	32.0	32.4	34.7
6	<i>cat-b</i>	Bz	Ph	0.0	21.5	18.5	10.8
ΔH_{298}							
2	<i>cat-b</i>	Me	Ph	0.0	24.2	21.4	19.1

^aFor the diastereomer assignment, the first and second letters refer to C2 and C3 of the products (Scheme 3). ^bThis reaction yields only one pair of enantiomers, e.g., both **TS-SS** and **TS-SR** lead to *S*-product.

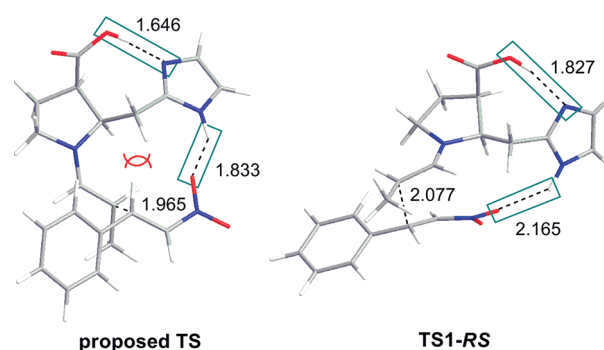


Figure 1. Proposed transition state and calculated lowest-energy transition state (**TS1-RS**) for Michael addition of propanal to nitrostyrene, catalyzed by *cat-a*. Hydrogen bonding and C \cdots C forming bond distances in Å.

(Figure 1), steric congestion around the α -methylene group is evidenced. Hence, we envisaged that better control of the hydrogen bonding network in the transition state is feasible by introducing a methyl group at the α position of the pyrrolidine ring, opposite to the designed hydrogen bonding network (*cat-b* in Scheme 3). The α -methyl substituent in *cat-b* is expected to serve two purposes: (1) enhance selectivity among various enamine conformers, which will be discussed later, and (2) balance out the steric effect exerted by the α -methylene group so that face selectivity of Michael addition would be dictated by a controlled hydrogen bonding as in our designed catalytic dyad.

Structures and Energies of Enamine Conformations. It is instructive to first examine various possible enamine conformers of catalysts *cat-a* and *cat-b* with propanal (**enam-a** and **enam-b**, respectively). Previous studies of aminocatalysis have shown that *E*-enamines are greatly preferred over *Z*-enamines because of their avoidance of unfavorable interaction between the substituent and the pyrrolidine ring.⁸ With respect to the C–N bond of enamine moiety, there are 2 possible geometrical arrangements, namely, *cis* and *trans*. For hydrogen bonding arrangement in enamine, there are open and stacked forms for the bridging type structures and conformation with a direct hydrogen bond between the carboxyl group and the enamine nitrogen

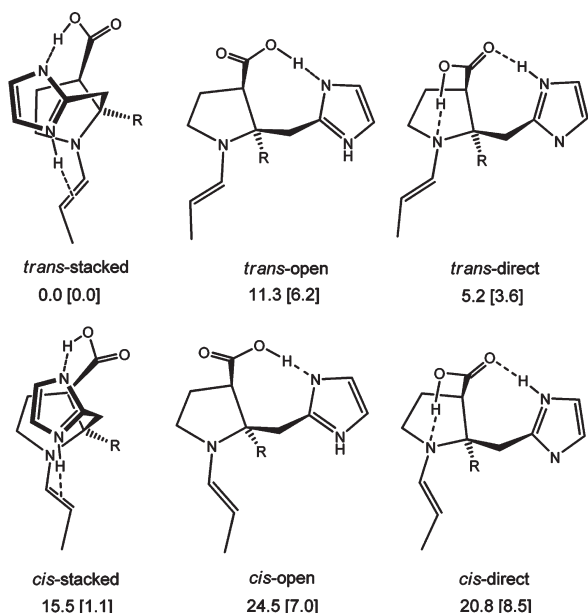


Figure 2. Various conformations of *E*-enamine intermediates, **enam-a** (R = H) and **enam-b** (R = Me). Calculated relative free energies (ΔG_{298} , kJ mol^{-1}), with the **enam-a** values in square brackets.

(Figure 2). As a result, there are 6 possible conformations of the *E* configuration of the enamines (Figure 2). Remarkably, the *trans*-stacked conformation, which features a stack arrangement between pyrrolidine and imidazole, is the most stable form. This preference is readily attributed to the steric repulsion exerted by the α -methyl and methylene groups and the favorable N–H $\cdots \pi$ interaction between the imidazole N–H and enamine π bond. The calculated N–H $\cdots \pi$ distance in *trans*-stacked **enam-b** is 2.64 Å. Weaker C–H $\cdots \pi$ and C–H \cdots N interactions between the two rings are also observed. Compared with **enam-a**, there is a stronger preference of the *trans*-stacked conformation in **enam-b**, which is readily attributed to the steric effect of the introduced α -methyl group.

cat-b-Catalyzed Michael Addition. As with **cat-a**, excellent enantio- and diastereoselectivity are also calculated for **cat-b**-catalyzed Michael addition with the same set of substrates (entry 2, Table 1). Surprisingly, **cat-b** is predicted to be highly *anti* diastereoselective (estimated *anti/syn* ratio $\sim 99:1$), in sharp contrast to the *syn* diastereoselectivity calculated for **cat-a**. This finding is highly interesting as there is no general *anti* protocol for amine-catalyzed conjugate additions with aldehyde donors,⁸ except for a recent elegant report by Uehara and Barbas.¹⁶ Organocatalysts based on a pyrrolidine template have long been known to catalyze nitro-Michael reaction of aldehydes. In 2001, Barbas reported the first example of asymmetric nitro-Michael reaction of aldehydes using (*S*)-(2-morpholinomethyl)-pyrrolidine as catalyst.¹⁷ Diastereoselectivities were generally good ($>85:15$), while only moderate enantioselectivities (56–78%) were obtained. In contrast, the simple catalyst L-proline was shown to be ineffective for this reaction, affording very low yield of the Michael products ($<5\%$ yield) and very poor enantioselectivity. Several highly efficient pyrrolidine-based organocatalysts have subsequently been reported, including diarylprolinol ethers (dr up to 95:5 and ee up to 99%),¹⁸ *N*-alkyl-2,2'-bipyrrrolidines (dr up to 95:5 and ee up to 96%),¹⁹ and *trans*-4-hydroxypropylamide (dr $> 90:10$, ee $>90\%$).²⁰ These

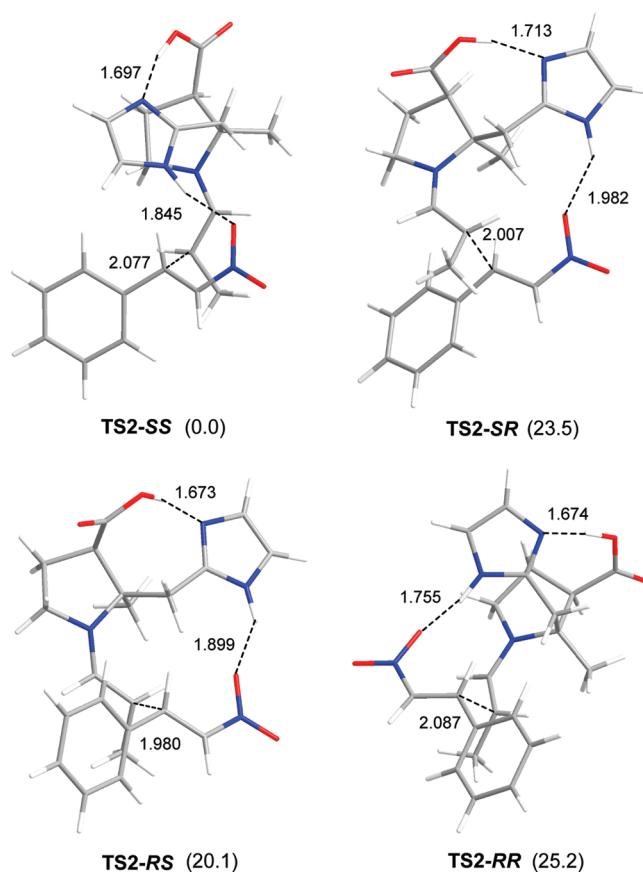


Figure 3. Optimized (M06-2X/6-31G**) geometries of the lowest energy transition states for the 4 possible diastereomeric products of **cat-b**-catalyzed conjugate addition of propanal to nitrostyrene. Hydrogen bonding and C \cdots C forming bond distances in Å. Calculated relative free energies (ΔG_{298} , kJ mol^{-1}) are given in parentheses.

organocatalysts typically promote *syn* Michael products. So far, no known organocatalysts based on pyrrolidine has been reported in literature that promotes *anti* nitro-Michael addition of aldehydes.

Figure 3 shows the 4 lowest-energy transition-state structures, namely, **TS2-SS**, **TS2-RR**, **TS2-SR** and **TS2-RS**, which produce the 4 different stereoisomeric products. The calculated activation barriers (ΔG_{298}^\ddagger), with respect to enamine + nitrostyrene, of the 4 transition states leading to the formation of (*S,S*), (*S,R*), (*R,S*), and (*R,R*) products are 38.6, 62.1, 58.7, and 63.8 kJ mol^{-1} , respectively. Formation of the (*2S,3S*) enantiomer, via **TS2-SS**, has the lowest activation barrier. It is worth noting that the computed relative enthalpies (ΔH_{298}) of the 4 key **TS2** transition states are very close to the corresponding relative free energies (ΔG_{298}) (Table 1). In other words, the entropy effects are similar for the 4 transition states. We have carried out benchmark calculations on the relative energies of the 4 transition states using a higher level of electron correlation treatment, at the CCSD level, and a larger basis set, up to the cc-pVTZ basis set. The results (Table S2, Supporting Information) suggest the level of theory (MP2/6-311+G**) employed in this study is sufficiently reliable.

Origin of Stereoselectivity. **TS2-SS** is derived from the *trans*-stacked enamine conformer, while the other 3 transition states, **TS2-RR**, **TS2-RS**, and **TS2-SR**, are derived from the higher-energy *cis*-open and *cis*-stacked conformers. It is remarkable that

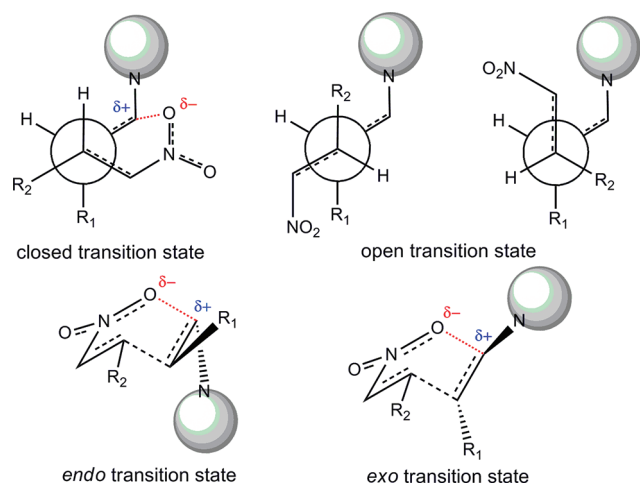


Figure 4. Definition of open and closed transition states and *endo* and *exo* forms of closed transition state in pyrrolidine-catalyzed Michael additions.

only one transition state derived from the lowest-energy *trans*-stacked conformer, i.e., **TS2-SS**, is relevant for the control of stereoselectivity of the reaction, but all other transition states derived from the same conformer are actually significantly higher in energy than those derived from other higher-energy enamine conformers. This excellent selectivity in transition states of the *trans*-stacked enamine conformer is attributed to 3 important factors: (1) the stacked conformation of the enamine moiety, (2) the introduction of the α -methyl group, and (3) our designed catalytic dyad via hydrogen bonding. Our calculations clearly show that the hydrogen bonding network between the imidazole ring and carboxyl group firmly stacked with the backbone of pyrrolidine ring in the *re* face, while the added methyl group blocks the *si* face. As a consequence, the *trans*-stacked *E*-enamine (Figure 2) has excellent *re* face selectivity. Together with the high directionality of our designed catalytic dyad, it is understandable why such high selectivity is observed for the *trans*-stacked conformer. In addition to the favorable geometry of the enamine moiety, **TS2-SS** avoids steric congestion at the α position of pyrrolidine backbone, as observed for 3 other higher-energy transition states (Figure 3).

It is intriguing to ask why *anti* selectivity is observed in our designed catalyst but not in most other organocatalysts reported in literature. Using the Heathcock model²¹ to construct various possible transition states, one may consider different approaches of the enamine to nitrostyrene by making 2 key assumptions: a closed transition state and a staggered conformation about the forming C···C bond. The closed transition state is defined by the six-membered ring, which includes the C=C double bond of enamine and C=C–N–O moiety of nitrostyrene, connected by the C···C forming bond and the C $_{\alpha}$ ···O attractive electrostatic interaction (see Figure 4). Essentially, the open and closed transition states differ only in the dihedral angles around the forming C···C bond. Here, we adopt the *endo/exo* notation to indicate the orientation of the pyrrolidine substituent with respect to the close transition structure (Figure 4). For pyrrolidine-catalyzed Michael additions, the most favorable transition states are always the *endo* transition states, which lead to *syn* products. In the *endo* transition state, electron donor enamine

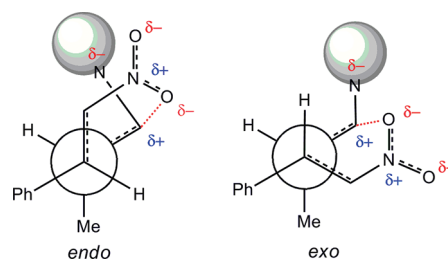
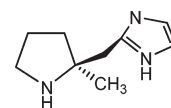


Figure 5. Schematic models of the *endo* and *exo* transition states for enamine organocatalysts.

nitrogen atom lies close to electron acceptor nitro group (Figure 5). Favorable electrostatic interaction stabilizes the *endo* configuration over the *exo* form. Additional hydrogen bonding stabilization is feasible if a hydrogen donor of the pyrrolidine ring is adjacent to the nitro group.

It is interesting to note that none of the **TS2** transition states (Figure 3) adopts an *endo* configuration. For the lowest-energy transition state **TS2-SS**, its unusual *exo* configuration leads to an *anti*-Michael adduct. To further shed light on the unusual adoption of an *exo* configuration in catalyst **cat-b**, the 2 lowest-energy *endo* transition states, namely, **TS2-SR'** and **TS2-SR''** (Figure 6), were investigated and compared with the *exo* **TS2-SS**. Indeed, both *endo* transition states are significantly higher in energy (by ~ 30 kJ mol⁻¹) than the *exo* **TS2-SS**. As evidenced in the optimized geometries, the COOH···N(imidazole) hydrogen bond of the catalytic dyad is disrupted in these *endo* transition states (Figure 6). More importantly, the nitro group is in direct close contact with the α -methylene group, causing significant steric repulsion. On the contrary, the *exo* **TS2-SS** maintains the catalytic dyad geometry and yet still avoids any unfavorable steric interaction with either the α -methyl or methylene group, albeit at the cost of losing some favorable electrostatic interaction. The key electrostatic interactions in the *endo* and *exo* transition states are supported by the calculated NBO atomic charges of **TS2-SR'** and **TS2-SR''** (Figure S1, Supporting Information).

cat-c-Catalyzed Michael Addition. It is crucial to establish the role of the carboxyl group of the coordinated catalytic dyad. To this end, we have investigated another catalyst, **cat-c**, in which the β -carboxyl group of **cat-b** is removed. The relative energies of the key transition states (**TS7**) for Michael addition of propanal to styrene catalyzed by **cat-c** are given in Table 2.



We note that there are 2 low-lying transition states, namely, **TS7-SR** and **TS7-SR'** (Figure 7), leading to the *syn* (2*S*,3*R*) product in this case. Comparing with **cat-b** (Table 1), the most obvious change in **cat-c** is the significant reduction of the relative energies of the two transition states leading to the *syn* product. Their energies are very close to that of **TS7-SS**, which leads to the *anti* product (2*S*,3*S*) (Table 2). The three transition states, however, feature hydrogen bonding patterns that differ greatly (Figure 7). This lack of selectivity and predictability of hydrogen bonding pattern in the computed transition states of **cat-c** provides strong

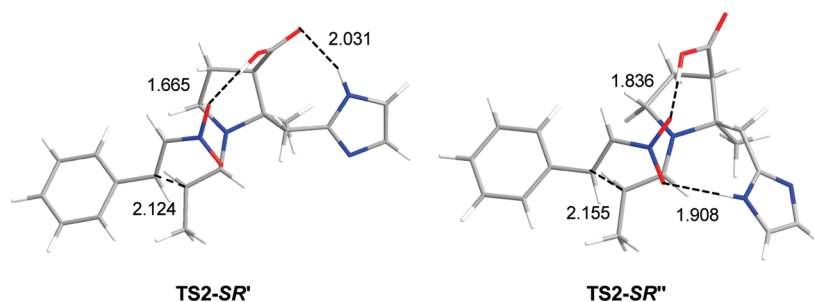


Figure 6. Optimized (M06-2X/6-31G**) geometries of *endo* transition states TS2-SR' and TS2-SR''.

Table 2. Calculated Relative Energies^a (ΔH_{298} and ΔG_{298} , kJ mol^{-1}) of the Four Lowest-Energy Transition States Leading to Four Stereoisomeric Products for cat-c-Catalyzed Michael Addition of Propanal to Nitrostyrene

transition state	ΔH_{298}	ΔG_{298}
TS7-SS	1.6	0.0
TS7-SR	1.3	2.3
TS7-SR'	0.0	2.7
TS7-RS	18.9	21.3
TS7-RR	20.2	22.4

^a MP2/6-311+G**//M06-2X/6-31G** level.

supporting evidence to our hypothesis that the β -carboxyl group in **cat-b** is important for the observed highly directional hydrogen bonding in TS2-SS. Furthermore, our calculations readily confirm that that β -carboxyl group is very important for the high *anti*-diastereoselectivity observed for **cat-b**. As noted in the discussion of **cat-b**-catalyzed reaction, adoption of an *endo* configuration in TS2-SR would disrupt the hydrogen bonding between the imidazole and carboxyl groups. This was cited as one of the plausible reasons for the observed preference for TS2-SS. Consequently, removing the β -carboxyl group from **cat-b** would lead to the release of this constraint on adopting the *endo* configuration and, thus, result in smaller relative energies of TS7-SR and TS7-SR' with respect to TS7-SS. Finally, we note that even without the constraint of the carboxyl/imidazole pair on adopting the *endo* configuration, TS7-SS is at least as stable as TS7-SR and TS7-SR'. This suggests that other controlling factor is in operation, most probably the steric congestion around the α position, exerted by the methylene group, which also impedes the adoption of an *endo* configuration but is also present in **cat-c**.

Substrate Scope and Solvent Effect. To investigate further the generality of the *anti* selectivity of **cat-b**, a substrate study was carried out for different aldehydes and nitroalkenes ($R^1 = \text{Me}$ or Bz , $R^2 = \text{H}$, Me , $i\text{Pr}$, or Ph , Scheme 3) at the same level of theory (MP2/6-311+G**//M06-2X/6-31G**). The calculated results are summarized in Table 1 (entries 3–6). In all cases, our designed catalyst **cat-b** promotes the (2*S*,3*S*) product with high enantio- and diastereoselectivity. Finally, we examined the effect of solvation on the predicted stereoselectivity. Implicit solvation method based on PCM¹² model was employed to investigate the effect of aprotic solvents, namely, chloroform and DMSO. No significant change in the preferred *anti* diastereoselectivity by **cat-b** in both solvents is observed (Table 3). Hence, our designed catalyst is a promising system for asymmetric catalysis. We realized that synthesis of the quaternary center in **cat-b** is not trivial. However, a literature search reveals that many efforts have

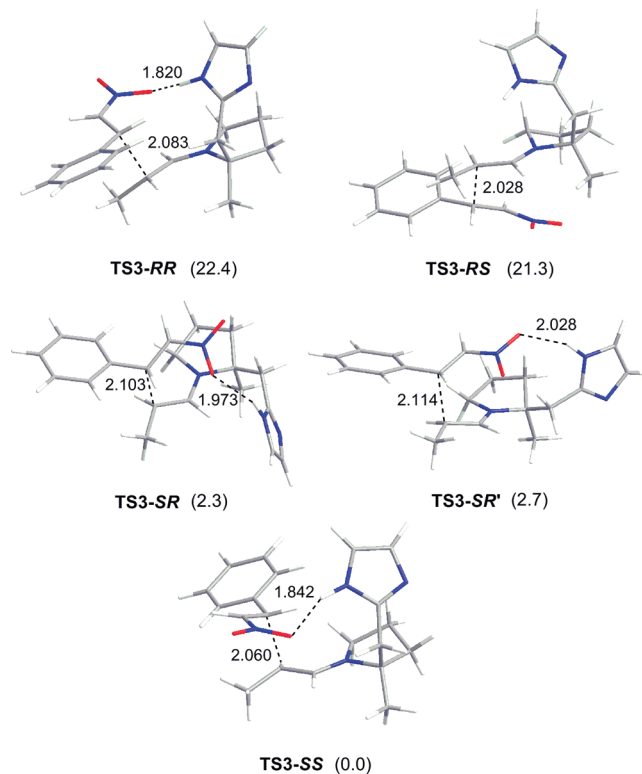


Figure 7. Optimized (M06-2X/6-31G**) geometries of the lowest energy transition states for the four possible diastereomeric products of **cat-c**-catalyzed conjugated addition of propanal to nitrostyrene. Hydrogen bonding and $\text{C}\cdots\text{C}$ forming bond distances in Å. Calculated relative free energies (ΔG_{298} , kJ mol^{-1}) are given in parentheses.

Table 3. Calculated Relative Free Energies^a (ΔG_{298} , kJ mol^{-1}) of the Four Lowest-Energy Transition States Leading to Four Stereoisomeric Products for **cat-b**-Catalyzed Michael Addition of Propanal to Nitrostyrene in Chloroform and DMSO Solvent

transition state	gas phase	chloroform	DMSO
TS2-SS	0.0	0.0	0.0
TS2-RS	23.5	20.8	21.0
TS2-SR	20.1	24.9	25.4
TS2-RR	25.2	25.9	26.3

^a MP2/6-311+G**//M06-2X/6-31G** level.

been devoted to quaternary center synthesis in recent years.²² In particular, the successful synthesis of analogues of **cat-b** by

Huang et al.²³ gives us confidence that **cat-b** can be easily synthesized.

CONCLUDING REMARKS

In conclusion, we have performed an *in silico* design of an organocatalyst using a bioinspired concept of catalytic carboxyl/imidazole dyad. We have shown that with appropriate steric control, our designed β -amino acid catalyst **cat-b** will react with simple aldehydes to form enamine intermediates with an unusual stacked conformation, which leads to highly organized and directional hydrogen bonding of the catalytic dyad in the transition states. When applied to the asymmetric nitro-Michael addition of aldehydes, **cat-b** promotes striking *anti* diastereoselectivity. In distinct contrast to Barbas's approach of using *Z*-enamine to promote *anti* selectivity,¹⁶ our designed catalyst makes use of *E*-enamine, which will provide a wider scope of general application. A remarkable substituent effect, namely, reversal of *syn/anti* selectivity, is predicted for the **cat-a/cat-b** catalyst pair. As mentioned in the Introduction, our proposed catalytic dyad is applicable to acid/base catalysis. We have performed preliminary calculations on a prototypical aldol reaction using the **cat-b** catalyst and obtained promising results. It is important to point out that the concept of catalytic dyad shall not be limited to the carboxyl/imidazole pair, as biochemistry has taught us. Although this study emphasizes the carboxyl/imidazole dyad, other combinations should be exploited in future studies of organocatalysis. Lastly, we note that β -amino acids are hardly employed as asymmetric organocatalysts.^{6b,24}

ASSOCIATED CONTENT

S Supporting Information. Complete ref 14; total energies and Cartesian coordinates of all optimized structures (Table S1); benchmark relative energies of various **TS2** transition states (Table S2); and NBO charges of selected transition states (Figure S1). This material is available free of charge via the Internet at <http://pubs.acs.org>.

AUTHOR INFORMATION

Corresponding Author

*E-mail: chmwmw@nus.edu.sg.

REFERENCES

- (1) (a) MacMillan, D. W. C. *Nature* **2008**, *455*, 304–308. (b) Dalko, P. I.; Moisan, L. *Angew. Chem., Int. Ed.* **2004**, *43*, 5138–517. (c) Berkessel, A.; Groeger, G. In *Asymmetric Organocatalysis: from Biomimetic Concepts to Applications in Asymmetric Synthesis*; Wiley-VCH: Weinheim, 2005. (d) Mukherjee, S.; Yang, J. W.; Hoffmann, S.; List, B. *Chem. Rev.* **2007**, *107*, 5471–5569. (e) List, B. *Tetrahedron* **2002**, *58*, 5573–5590.
- (2) List, B.; Lerner, R. A.; Barbas, C. F., III *J. Am. Chem. Soc.* **2000**, *122*, 2395–2396.
- (3) (a) Calderon, F.; Doyaguez, E. G.; Cheong, P. H.; Fernandez-Mayoralas, A.; Houk, K. N. *J. Org. Chem.* **2008**, *73*, 7916–7920. (b) Bahmanyar, S.; Houk, K. N. *J. Am. Chem. Soc.* **2001**, *123*, 12911–12912. (c) Rankin, K. N.; Gauld, J. W.; Boyd, R. J. *J. Phys. Chem. A* **2002**, *106*, 5155–5159.
- (4) (a) Garrett, R. H.; Grisham, C. M. *Biochemistry*, 4th ed.; Brooks/Cole, Cengage Learning: Boston, 2010; pp 434–439. (b) Kasserra, H. P.; Laidler, K. J. *Can. J. Chem.* **1969**, *47*, 4031–4039.
- (5) (a) Kona, J. *Org. Biomol. Chem.* **2008**, *6*, 359–365. (b) Menard, R.; Khouri, H. E.; Plouffe, C.; Laflamme, P.; Dupras, R.; Vernet, T.; Tessier, D. C.; Thomas, D. Y.; Storer, A. C. *Biochemistry* **1991**,

30, 5531–5538. (c) Khersonsky, O.; Tawfik, D. S. *J. Biol. Chem.* **2006**, *281*, 7649–7656. (d) Schultz, L. W.; Quirk, D. J.; Raines, R. T. *Biochemistry* **1998**, *37*, 8886–8898. (e) Botos, I.; Melnikov, E. E.; Cherry, S.; Tropea, J. E.; Khalatova, A. G.; Rasulova, F.; Dauter, Z.; Maurizi, M. R.; Rotanova, T. V.; Wlodawer, A.; Gustchina, A. *J. Biol. Chem.* **2004**, *279*, 8140–8148. (f) Raber, M. L.; Arnett, S. O.; Townsend, C. A. *Biochemistry* **2009**, *48*, 4959–4971.

(6) (a) Houk, K. N.; Cheong, P. H. *Nature* **2008**, *455*, 309–313. (b) Mitsumori, S.; Zhang, H.; Cheong, P. H.; Houk, K. N.; Tanaka, F.; Barbas, C. F., III *J. Am. Chem. Soc.* **2006**, *128*, 1040–1041. (c) Fleming, E. M.; Quigley, C.; Rozas, I.; Connon, S. J. *J. Org. Chem.* **2008**, *73*, 948–956. (d) Shinisha, C. B.; Sunoj, R. B. *Org. Biomol. Chem.* **2007**, *5*, 1287–129.

(7) Armstrong, A.; Bhonoah, Y.; White, A. J. P. *J. Org. Chem.* **2009**, *74*, 5041–5048.

(8) Pihko, P. M.; Majander, I.; Erkila, A. *Top. Curr. Chem.* **2009**, *291*, 29–74.

(9) For examples, see: (a) Melchiorre, P.; Jorgensen, K. A. *J. Org. Chem.* **2003**, *68*, 4151–4157. (b) Hoang, L.; Bahmanyar, S.; Houk, K. N.; List, B. *J. Am. Chem. Soc.* **2003**, *125*, 16–17. (c) List, B.; Hoang, L.; Martin, H. J. *Proc. Natl. Acad. Sci. U.S.A.* **2004**, *101*, 5839–5842. (d) Shinisha, C. B.; Sunoj, R. B. *Angew. Chem., Int. Ed.* **2010**, *49*, 6373–6377.

(10) Calderon, F.; Doyaguez, E. G.; Cheong, P. H.; Fernandez-Mayoralas, A.; Houk, K. N. *J. Org. Chem.* **2008**, *73*, 7916–7920.

(11) Zhao, Y.; Truhlar, D. G. *Theor. Chem. Acc.* **2008**, *120*, 215–241.

(12) (a) Cossi, M.; Barone, V.; Cammi, R.; Tomasi, J. *Chem. Phys. Lett.* **1996**, *255*, 327–355. (b) Barone, V.; Cossi, M.; Tomasi, J. *J. Chem. Phys.* **1997**, *107*, 3210–3221.

(13) Reed, A. E.; Curtiss, L. A.; Weinhold, F. *Chem. Rev.* **1988**, *88*, 899–926.

(14) Frisch, M. J. et al. *Gaussian 09*, Revision A.02; Gaussian, Inc.: Wallingford, CT, 2009.

(15) For reviews on asymmetric organocatalytic Michael reactions, see: (a) Tsogoeva, S. B. *Eur. J. Org. Chem.* **2007**, 1701–1716. (b) Vicario, J. L.; Badia, D.; Carrillo, L. *Synthesis* **2007**, 2065–2092. (c) Sulzer-Mossé, S.; Alexakis, A. *Chem. Commun.* **2007**, 3123–3135. (d) Notz, W.; Tanaka, F.; Barbas, C. F., III *Acc. Chem. Res.* **2004**, *37*, 580–591.

(16) Uehara, H.; Barbas, C. F., III *Angew. Chem., Int. Ed.* **2009**, *48*, 9848–9852.

(17) Betancort, J. M.; Barbas, C. F., III *Org. Lett.* **2001**, *3*, 3737–3740.

(18) Palomo, C.; Mielgo, A. *Angew. Chem., Int. Ed.* **2006**, *45*, 7876–7880.

(19) Andrey, O.; Alexakis, A.; Tomassini, A.; Bernardinelli, G. *Adv. Synth. Catal.* **2004**, *346*, 1147–1168.

(20) Palomo, C.; Vera, S.; Mielgo, A.; Gomez-Bengoia, E. *Angew. Chem., Int. Ed.* **2006**, *45*, 5984–5987.

(21) Oare, D. A.; Heathcock, C. H. In *Topics in Stereochemistry*; Eliel, E. L., Wilen, S. H., Eds.; Wiley: New York, 1989; Vol. 19, pp 227–408.

(22) Seebach, D. *Angew. Chem., Int. Ed.* **2011**, *50*, 96–101.

(23) Xiao, K.; Luo, J.; Ye, K.; Wang, Y.; Huang, P. *Angew. Chem., Int. Ed.* **2010**, *49*, 3037–304.

(24) (a) Davies, S. G.; Russell, A. J.; Sheppard, R. L.; Smith, A. D.; Thomson, J. E. *Org. Biomol. Chem.* **2007**, *5*, 3190–3200. (b) Limbach, M. *Tetrahedron Lett.* **2006**, *47*, 3843–3847.